Gut microbiota and their metabolite profiles following peripheral nerve xenotransplantation

Yongsheng Chen [a], Huihui Chai [b], Zhenzhen Li [a], Bin Liu [a], Minxuan Tan [a], Shaopeng Li [a,**], Yanxia Ma [c,d,e,*]

[a] Department of Neurosurgery, Dongguan People's Hospital (Affiliated Dongguan Hospital, Southern Medical University), Dongguan, Guangdong, China
[b] Department of Cerebrovascular Surgery, The Third Affiliated Hospital of Sun Yat-Sen University, Guangzhou 510360, Guangdong, China
[c] Department of Neurosurgery, The National Key Clinical Specialty, Zhujiang Hospital of Southern Medical University, Guangzhou, Guangdong, China
[d] Department of Neurosurgery, The Engineering Technology Research Center of Education Ministry of China, Zhujiang Hospital of Southern Medical University, Guangzhou, Guangdong, China
[e] Department of Neurosurgery, Guangdong Provincial Key Laboratory on Brain Function Repair and Regeneration, Zhujiang Hospital of Southern Medical University, Guangzhou, Guangdong, China

ARTICLE INFO

ABSTRACT

Background: Intestinal pathogens are associated with xenotransplantation tolerance and rejection. However, changes in the gut microbiota in patients who have undergone peripheral nerve xenotransplantation and their association with immune rejection have not yet been reported.
Objective: We aimed to explore intestinal microbes and their metabolites at different time points after peripheral nerve transplantation to provide new insight into improving transplant tolerance.
Methods: A peripheral nerve xenotransplantation model was constructed by suturing the segmented nerves of Sprague Dawley rats to those of C57 male mice using xenotransplantation nerve bridging. Fecal samples and intestinal contents were collected at three time points: before surgery (Pre group; n = 10), 1 month after transplantation (Pos1 m group; n = 10), and 3 months after transplantation (Pos3 m group; n = 10) for 16S DNA sequencing and nontargeted metabolome detection.
Results: Alpha diversity results suggested that species diversity was significantly downregulated after peripheral nerve xenotransplantation. There were six gut flora genera with significantly different expression levels after xenotransplantation: four were downregulated and two were upregulated. A comparison of the Pre vs. Pos1 m groups and the Pos1 m vs. Pos3 m groups revealed that the most significant differentially expressed Kyoto Encyclopedia of Genes and Genomes metabolite pathways were involved in phenylalanine, tyrosine, and tryptophan biosynthesis, as well as histidine metabolism. Metabolites with a strong relationship to the differentially expressed microbial flora were identified.
Conclusion: Our study found lower gut microbiome diversity, with increased short-chain fatty acid (SCFA)-producing and sulfate-reducing bacteria at 1 month post peripheral nerve

---

* Corresponding author. Department of Neurosurgery, The National Key Clinical Specialty, Zhujiang Hospital of Southern Medical University, Guangzhou, Guangdong, China.
** Corresponding author. Department of Neurosurgery, Puji Branch of Dongguan People's Hospital (Affiliated Dongguan Hospital, Southern Medical University), No.1 Guangmingxin Street, Dongcheng District, Dongguan 523000, Guangdong Province, China.
E-mail addresses: Shaopengli666@126.com (S. Li), Laoma888xin@sina.com (Y. Ma).

xenotransplantation, and these were decreased at 3 months post-transplantation. The identification of specific bacterial metabolites is essential for recognizing potential diagnostic markers of xenotransplantation rejection or characterizing therapeutic targets to prevent post-transplant infection.

1. Introduction

Peripheral nerve injuries are caused by common diseases that directly or indirectly injure a peripheral nerve, resulting in motor and sensory disorders. Autologous nerve transplantation is limited due to the need for a secondary surgery to harvest graft tissue from a healthy nerve [1–3]. Thus, xenotransplantation with donor nerve tissue is used as an alternative to autologous nerve grafts [4]. However, immunological barriers limit the application of xenotransplantation, with three main types of rejection: hyperacute xenograft rejection, acute humoral xenograft rejection, and acute cellular rejection [5]. Understanding the pathogenesis of xenotransplantation rejection is key to determining the safety and viability of xenotransplantation in clinical applications.

The disordered gut microbiota, characterized by loss of microbiome diversity, reduced abundance, and pathogenic outgrowth, is involved in a variety of host physiological processes [6]. More importantly, gut microbial dysbiosis is linked to an aberrant immune response, often accompanied by abnormal production of inflammatory cytokines. A comparative study on germ-free (GF) mice and specific pathogen-free mice revealed that the number of T-cell receptors on γδ intraepithelial lymphocytes was decreased in GF mice [7]. Melanie revealed the association of tumor necrosis factor α and interferon γ production with specific microbial metabolic pathways [8].

Dysfunctional intestinal flora may activate host immune responses via metabolites produced by the gut microbiota axis [9,10]. Since allogeneic transplantation (e.g., hematopoietic stem cell, kidney, liver, and small bowel transplantation) decreases the population and diversity of intestinal microbes, this may be the main cause of postoperative complications in transplantation surgery (including graft-versus-host disease [GVHD], relapse, and infection), leading to increased mortality [6,11–13]. The important influence of intestinal microbiota on the immune response has become increasingly recognized, and the gut is one of the main targets of acute GVHD. A number of publications have demonstrated the association of a dysbiotic microbiome with GVHD. Marina found that GVHD patients had a lower abundance of members of the class Clostridia, lower counts of butyrate producers, and lower ratios of strict to facultatively anaerobic bacteria compared with allograft recipients who did not have GVHD [14]. The regulation of the immune response by intestinal flora affects a patient's prognosis and has been reported in hematopoietic stem cell transplantation [15]. Although most bacteria colonize the intestinal lumen, segmented filamentous bacteria can penetrate the mucus layer, stimulate epithelial cells, and induce T helper (Th) 17 cell differentiation. The Th17 cells secrete cytokines, such as interleukin (IL)-17A, IL-17F, IL-21, and IL-22, which exert an antibacterial effect [16]. Except for allogeneic donor T-cells, recipient-derived myeloid cells (including neutrophils and inflammatory monocytes) are also involved in gastrointestinal damage in allogeneic hematopoietic stem cell transplantation [17,18]. Studies have suggested that regulating the RIG-I/MAVS and STING signaling pathways promotes intestinal tract integrity in mice with hematopoietic stem cell transplantation [19]. Moreover, short-chain fatty acids (SCFAs) produced by some bacteria were considered to be involved in both innate and adaptive immunity [20]. Immune responses following discordant xenotransplantation include both acquired immunity and innate immunity, in which natural antibodies, complement, natural killer cells, and macrophages play interdependent roles. Roland investigated the initial human pan-T-cell reaction in a cardiac xenotransplant model and found that contact between human blood and pig endothelium activates cytotoxic T-cells within the first few hours, indicating acute rejection [21]. However, alteration of the recipient's gut microbiota and its correlation with immune rejection in peripheral nerve xenotransplantation has yet to be reported.

Our previous research revealed that an imbalance between regulatory T-cells (Tregs) and Th1–Th17–Th22 cells contributed to the acute rejection of peripheral nerve xenotransplants and was modulated by Treg-Th1-Th17-Th22 cells [22]. Here, we aim to describe the alteration in intestinal microbes and metabolites following xenograft peripheral nerve transplantation to explore the correlation between microbes and their metabolites and immune rejection, providing new insights into the mechanism of complications in peripheral nerve transplantation.

2. Methods

2.1. Preparation of a mouse model of peripheral nerve xenotransplantation

The peripheral nerve xenotransplantation model was constructed as previously described [22] using 10 adult male Sprague Dawley (SD) rats and 30 healthy 5–10-week-old C57 BL/6 male mice as donors and recipients, respectively. The experiment was approved by the ethical committee of Guangzhou Forevergen Biosciences (Guangzhou, China) (approval number IACUC-AEWC-F2006012). Sciatic nerves of SD rats were exposed under aseptic surgical conditions, cut into 1-cm segments, and then stored at −80 °C for later use. Fecal samples were randomly collected from 10C57 mice for 16S DNA sequencing and liquid chromatography-tandem mass spectrometry (LC-MS/MS) analysis. We then anesthetized the recipient C57 mice, removed a segment of the sciatic nerve, and sutured the segmented nerves of SD rats to the C57 mice using xenotransplantation nerve bridging. Fecal samples were randomly collected from 10 mice at 1 month post-surgery (Pos1 m; n = 10) and at 3 months post-surgery (Pos3 m; n = 10).

2.2. 16S DNA sequencing

Total DNA was extracted from the fecal samples using a DP328 DNA extraction kit according to the manufacturer's instructions (Tiangen Biotech, Beijing, China). Polymerase chain reaction amplification was performed with primers designed to target a conserved region, and the resultant product was purified, quantified, and homogenized for library construction. The qualified library was sequenced on an Illumina HiSeq 2500 platform (Novogene, Beijing, China). The original data obtained by high-throughput sequencing was converted into sequenced reads using base calling analysis.

2.3. LC-MS/MS analysis

The metabolites were extracted using 500 μL extraction solution (methanol:acetonitrile:water = 2:2:1) (v/v/v), and the supernatant was collected at 13,800×g for 15 min at 4 °C. The samples were analyzed using a Vanquish ultra-high performance liquid chromatography system (Thermo Fisher Scientific, Guangzhou,China) with a UPLC BEH Amide Column (2.1 mm × 100 mm, 1.7 μm) coupled to a Q Exactive HF-X Orbitrap mass spectrometer (Thermo Fisher Scientific). The mobile phase consisted of either 25 mmol/L ammonium acetate and 25 ammonia hydroxide in water (pH = 9.75) (A) or acetonitrile (B). The auto-sampler temperature was 4 °C, and the sample volume was 3 μL.

The mass spectrometer was used to collect MS/MS spectra in information-dependent acquisition mode using Xcalibur acquisition software (Thermo Fisher Scientific). In this mode, the acquisition software continuously evaluates the full scan MS spectrum. The electrospray ionization source was set as follows: sheath gas flow rate, 30 Arb; Aux gas flow rate, 25 Arb; capillary temperature, 350 °C; full MS resolution, 60000; MS/MS resolution, 7500; collision energy, 10/30/60 in normalized collision energy mode; and spray voltage, 3.6 kV (positive) or −3.2 kV (negative).

2.4. Metabolomics analysis

The raw data were converted to mzXML format with ProteoWizard software and processed for peak detection, extraction, alignment, and integration. Metabolite annotation was then performed using an in-house MS2 database (BiotreeDB) with the cutoff value set at 0.3. SIMCA software v16.0.2 (Sartorius Stedim Data Analytics AB, Umea, Sweden) was then used to perform logarithmic conversion and UV formatting, principal coordinates analysis (PCoA), and orthogonal partial least squares method-discriminant analysis. The differentially expressed metabolites were then analyzed using a volcano plot. Next, the candidate differentially expressed metabolites were used for Kyoto Encyclopedia of Genes and Genomes (KEGG) pathway analysis. Finally, we performed pairwise correlation to identify the correlation between specific microbiota and metabolites based on the Pearson correlation coefficient (r) and p-value.

2.5. Statistical analysis of microbial data

We used Trimmomatic v0.33 to filter the raw reads and obtained clean reads after removing the primer sequence. Operational taxonomic units (OTUs) were obtained by clustering clean reads at a similarity level of 97.0%. Chao index and Shannon index were
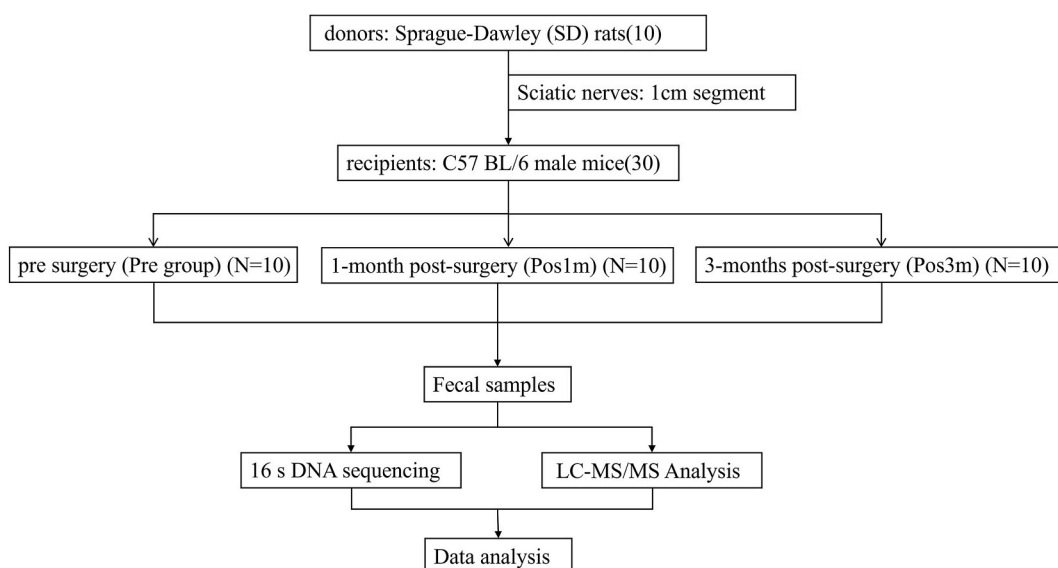

Fig. 1. Flowchart of our study.

selected to reflect the alpha diversity of the samples. A heatmap was used for microbiota clustering according to the species abundance. The linear discriminant analysis effect size (LEfSe) was adopted for detecting the differences in species composition and communities among groups. A Venn diagram was used to show the number of common and unique features between different groups. Repeated measures ANOVA and rank sum test were used to analyze the expression levels among groups. Bonferroni multiple-comparison method was used for the comparison of means in Chao index and Shannon index. All statistical analyses were performed using SPSS v22.0 (IBM Corp., Armonk, IL, USA), with $p < 0.05$ considered statistically significant.

3. Results

3.1. Reduced alpha diversity after peripheral nerve transplantation

Flowchart of our study was showed in Fig. 1. Then, we focus the results of Gut microbiota. The OTUs of all samples ranged from 335 to 413, with proper uniformity (Fig. 2A). The mutual number of OTUs among the Pre, Pos1 m, and Pos3 m groups was 439 (Fig. 2B). Alpha diversity was performed to analyze the richness and uniformity of species composition, including Chao index (abundance of the community in the sample) and Shannon index (abundance and uniformity of species). There were no significant differences in the Chao index among the Pre, Pos1 m, and Pos3 m groups, suggesting that xenotransplantation did not affect the species abundance of the recipient's intestinal flora (Fig. 2C). Shannon index was significantly reduced at 3 months after transplantation, suggesting that species diversity was significantly downregulated after peripheral nerve xenotransplantation ($p < 0.001$) (Fig. 2D).

3.2. Microbial flora identification in peripheral nerve xenotransplantation

PCoA based on the unweighted UniFrac distance showed that the microbial flora in the Pos1 m and Pos3 m groups were significantly different, with a certain overlap before and after peripheral nerve xenotransplantation (Fig. 3A). The microbiota abundance from phylum to genus levels differed significantly among the three groups. The dominant intestinal flora included Bacteroidetes, Firmicutes, Verrucomicrobia, and Actinomycetes at the phylum level (Fig. 3B) and *Muribaculaceae*, *Ruminococcaceae*, *Akkermansia*, *Lachnospiraceae*, and *Desulfovibrio* at the genus level (Fig. 3C).
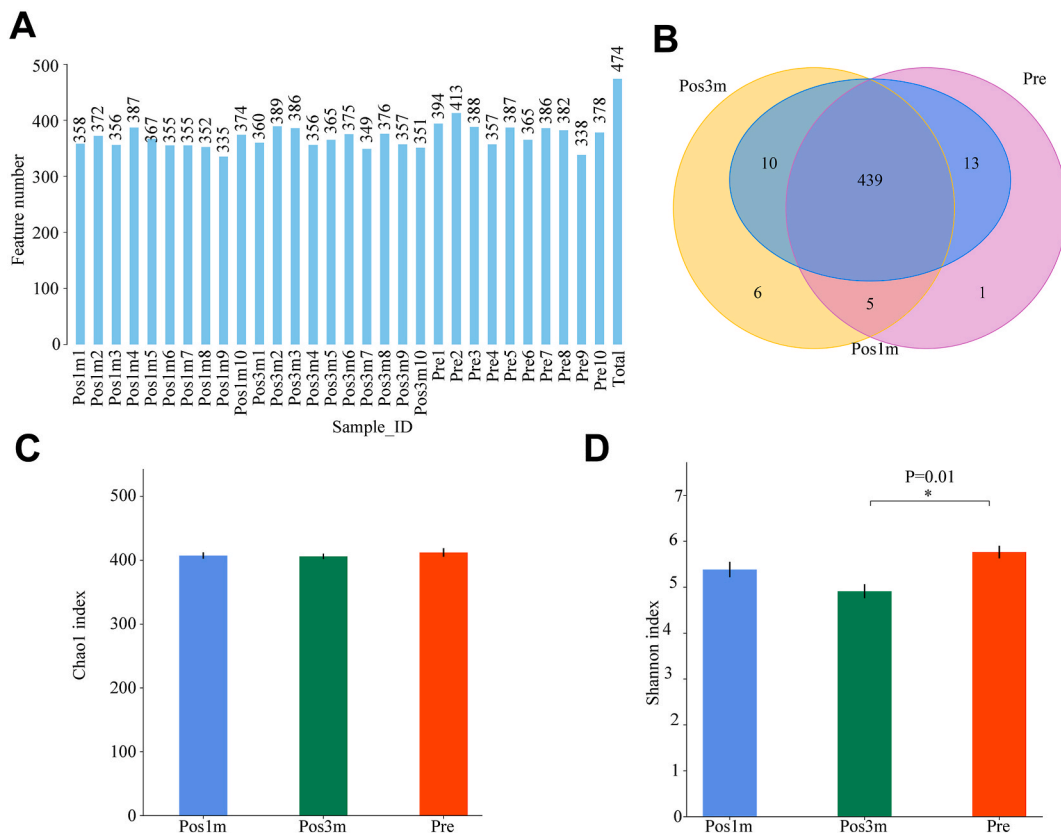

Fig. 2. 16S data overview. A. The OTUs of all samples range from 335 to 413; **B.** The mutual number of OTUs among the Pre, Pos1 m, and Pos3 m groups is 439; **C.** There is no significant difference in Chao index among the Pre, Pos1 m, and Pos3 m groups; **D.** Shannon index was significantly reduced at 3 months after peripheral nerve xenotransplantation. *$p < 0.05$.

3.3. Differential microbial expression after peripheral nerve xenotransplantation

Linear discriminant analysis (LDA) results meeting the criteria of an LDA score >4.0 with a p-value <0.05 were used to estimate changes in species abundance. The higher the LDA score, the greater the effect of the microbiota on the peripheral nerve xeno-transplantation among the three groups (Fig. 4A). Significantly expressed species before and after peripheral nerve xeno-transplantation were identified by LEfSe analysis. Specifically, uncultured_bacterium_g_*Lachnospiraceae*_NK4A136_group, g_*Lachnospiraceae*_NK4A136_group, and o_Clostridiales were more abundant in the Pos1 m group, and s_uncultured_bacter-ium_g_*Akkermansia*, g_*Akkermansia*, f_*Akkermansiaceae*, and o_Verrucomicrobiales were more abundant in the Pos3 m group, while s_uncultured_bacterium_g_*Ruminococcaceae*_UCG_004, g_*Ruminococcaceae*_UCG_004, f_*Ruminococcaceae*, s_uncultured_bacter-ium_g_*Dubosiella*, g_*Dubosiella*, s_uncultured_bacterium_g_*Faecalibaculum*, g_*Faecalibaculum*, f_*Erysipelotrichaceae*, o_Erysipelotrichaceae s_uncultured_bacterium_g_*Desulfovibrio*, g_*Desulfovibrio*, f_Desulfovibrionaceae, and o_Desulfovibrionales were more abundant in the Pre group (Fig. 4B). There were six differentially expressed microbes at the genus level, four of which were downregulated (*Desul-fovibrio*, *Dubosiella*, *Faecalibaculum*, and *Ruminococcaceae*) and two of which were upregulated (*Akkermansia* and *Lachnospiraceae*) (Fig. 4C).

3.4. Differentially expressed metabolites and their predicted functional pathways

We used nontarget metabolome analysis to explore the functional role of different microorganisms. PCoA based on the unweighted UniFrac distance showed no significant aggregation among the Pre, Pos1 m, and Pos3 m groups (Fig. 5A). In the volcano plot, with p-values <0.05 considered statistically significant, there were 181 upregulated and 86 downregulated metabolites identified between the Pre and Pos1 m groups (Fig. 5B) and 2625 upregulated and 1992 downregulated metabolites between the Pre and Pos3 m groups (Fig. 5C). The KEGG pathways of differentially expressed metabolites between the Pre and Pos1 m groups showed significant enrichment of phenylalanine, tyrosine, and tryptophan biosynthesis; D-glutamine and D-glutamate metabolism; cysteine and methi-onine metabolism; pantothenate and coenzyme A biosynthesis; valine, leucine, and isoleucine biosynthesis; and phenylalanine metabolism (Fig. 5D). The KEGG pathways of differentially expressed metabolites between the Pos1 m and Pos3 m groups were significantly enriched in histidine metabolism and vitamin B6 metabolism (Fig. 5E).

3.5. Correlation analysis of differentially expressed microbiota and metabolites

A total of 18 metabolites met the criteria of a variable importance in projection >1 and a p-value <0.05 and were considered differentially expressed metabolites. The top 5 upregulated and top 5 downregulated metabolites from Pre vs. Pos1 m and Pre vs. Pos3 m were chosen for correlation analysis with microbial flora (two recurring microorganisms were removed). The heatmap showed a significant correlation between different flora and differentially expressed metabolites after xenotransplantation, proving that nerve xenotransplantation changes the composition of intestinal flora and further affects the metabolic expression spectrum of intestinal flora. *Akkermansia* was positively correlated with (2E)-decenoyl-ACP. *Faecalibaculum* was positively correlated with (x)-1,2-Pro-panediol 1-O-b-D-glucopyranoside, tetracosahexaenoic acid (THA; 24:6n-3), melilotoside C, phlorizin, and 2-hexaprenyl-3-methyl-6-methoxy-1,4 benzoquinone and negatively correlated with PE(20:4(5Z, 8Z, 11Z, 14Z)/15:0) and medicanine. *Dubosiella* was positively correlated with (2E)-decenoyl-ACP, suspensolide F, and melilotoside C and negatively correlated with medicanine. *Ruminococca-ceae*_UCG-004 was positively correlated with THA, stigmast-22-ene-3,6-dione, monocrotaline, and 2-hexaprenyl-3-methyl-6-methoxy-1,4 benzoquinone and negatively correlated with rotenone and PE (20:4(5Z, 8Z, 11Z, 14Z)/15:0). *Desulfovibrio* was positively correlated with medicanine, stigmast-22-ene-3,6-dione, and (2E)-N-(4-aminobutyl)-3-(4-hydroxy-3-methoxyphenyl)prop-2-enimidic acid and negatively correlated with (2E)-decenoyl-ACP and suspensolide F (Fig. 6).
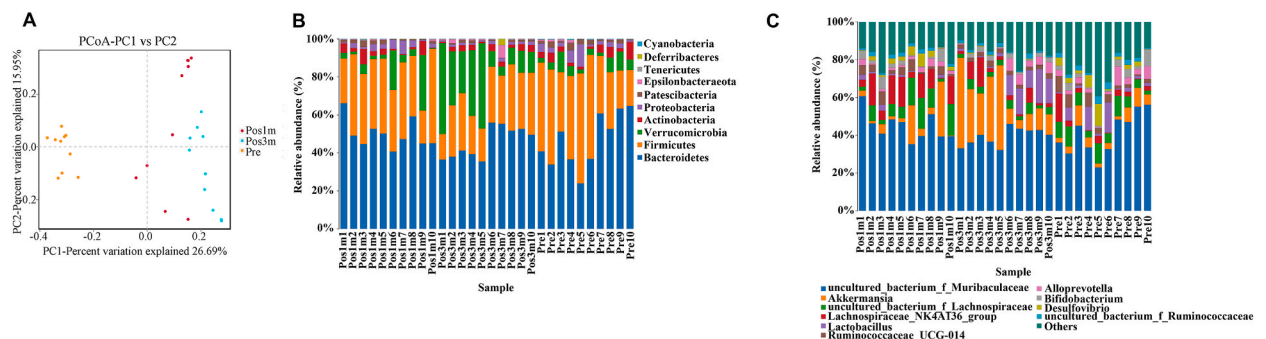

Fig. 3. Dominant microbial flora before and after peripheral nerve xenotransplantation. A. PCoA showed that the microbial flora were significantly different, with a certain overlap between the Pos1 m and Pos3 m groups before and after peripheral nerve xenotransplantation; **B.** The top 10 dominant intestinal flora at the phylum level include Bacteroidetes, Firmicutes, Verrucomicrobia, and Actinomycetes; **C.** The top 10 dominant intestinal flora at the genus level include *Muribaculaceae*, *Ruminococcaceae*, *Akkermansia*, *Lachnospiraceae*, and *Desulfovibrio*.
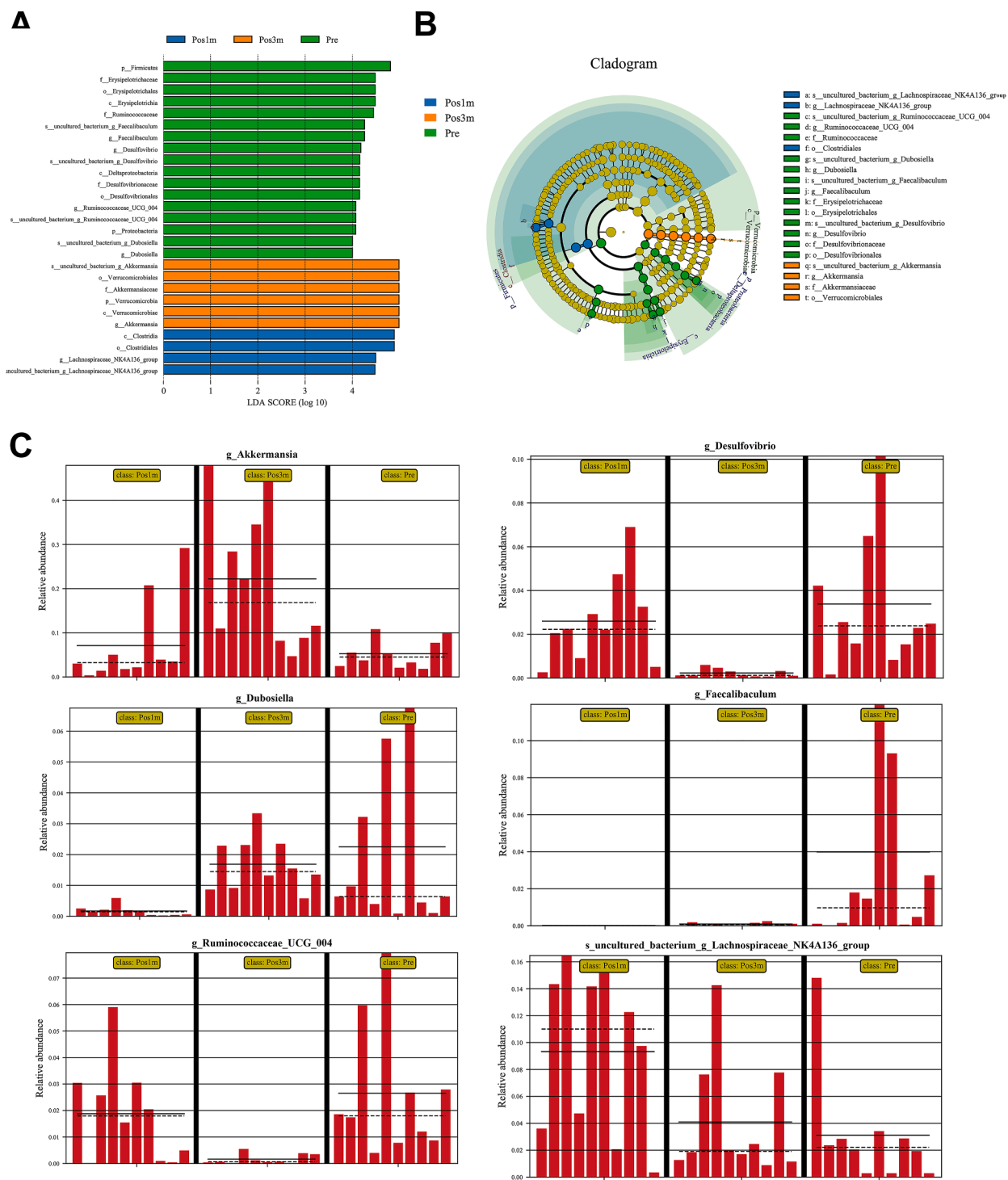
Fig. 4. Differential microbial analysis. A. Linear discriminant analysis (LDA) score. LDA results fulfilling the criteria of an LDA score >4.0 with a p-value <0.05 are shown; **B.** LEfSe clustering tree demonstrating the differences in bacterial abundance between the Pre, Pos1 m, and Pos3 m groups. Each colored circle represents a biomarker, and the diameter of the circle is proportional to the relative abundance. Yellow nodes represent microbial groups with no significant differences. Nodes of different colors indicate different microbial groups that play an important role in the group; **C.** Six differentially expressed microbes were found at the genus level, with four downregulated and two upregulated. (For interpretation of the references to color in this figure legend, the reader is referred to the Web version of this article.)
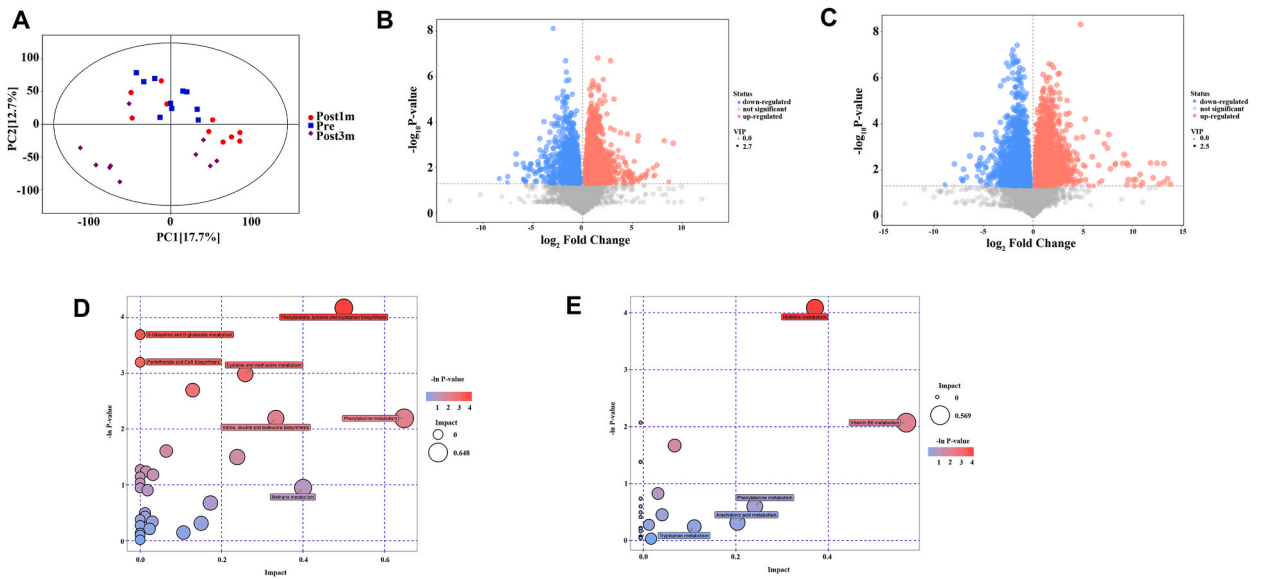
Fig. 5. Differentially expressed metabolites and the predicted signal pathways. A. PCoA showed no significant aggregation among the Pre, Pos1 m, and Pos3 m groups; **B.** The volcano plot showed significant differentially expressed metabolites between the Pre and Pos1 m groups. Each dot represents a metabolite. Red dots are upregulated metabolites, blue dots are downregulated metabolites, and gray dots are metabolites with no significant differences; **C.** The volcano plot showed significant differentially expressed metabolites between the Pre and Pos3 m groups. Each dot represents a metabolite. Red dots are upregulated metabolites, blue dots are downregulated metabolites, and gray dots are metabolites with no significant differences; **D.** The KEGG pathways of differentially expressed metabolites between the Pre and Pos1 m groups; **E.** The KEGG pathways of differentially expressed metabolites between the Pos1 m and Pos3 m groups. (For interpretation of the references to color in this figure legend, the reader is referred to the Web version of this article.)

4. Discussion

The further development of peripheral nerve xenotransplantation is mainly hampered by complications that are closely related to the host's immune system, specifically involving intestinal microflora [23]. Our alpha diversity results suggest that species diversity is significantly downregulated after peripheral nerve xenotransplantation. We found six gut microbes with significantly differentiated expression levels after xenotransplantation; four were downregulated (*Desulfovibrio*, *Dubosiella*, *Faecalibaculum*, and *Ruminococcaceae*) and two were upregulated (*Akkermansia* and *Lachnospiraceae*). The most significant KEGG pathways of differentially expressed metabolites of Pre vs. Pos1 m and Pos1 m vs. Pos3 m were significantly enriched in phenylalanine, tyrosine, and tryptophan biosynthesis and histidine metabolism. Metabolites strongly associated with the differentially expressed microbial flora included (2E)-decenoyl-l-ACP, suspensolide F, rotenone, PE(20:4(5Z, 8Z, 11Z, 14Z)/15:0), medicanine, THA, melilotoside C, stigmast-22-ene-3,6-dione, and 2-hexaprenyl-3-methyl-6-methoxy-1,4 benzoquinone.

The intestinal microbiota includes over 1000 different species, and dysregulation of the gut microbiota composition and diversity has been associated with diet, antibiotics, and the immune system [24,25]. Rapid shifts in intestinal microbial composition and diversity lead to dysbiosis, contributing to the development of diseases such as GVHD [17]. A decreased abundance of microbial flora reduces the inflammatory response [26], and this correlated with our findings of a significant downregulation of species diversity after peripheral nerve xenotransplantation. This characterization of intestinal dysbiosis is an essential prerequisite to better understanding the impact of microbiota on xenotransplantation.

We observed six intestinal flora with significantly different expression levels. *Desulfovibrio*, *Dubosiella*, *Faecalibaculum*, and *Ruminococcaceae* were downregulated and *Akkermansia* and *Lachnospiraceae* were upregulated. *Akkermansia* is an intestinal symbiont bacterium of the mucosal layer that degrades intestinal mucus, thereby improving host metabolic functions and immune responses [27]. A significant increase in *Akkermansia* was reported in dextran sulfate sodium-induced colon inflammation, suggesting that *Akkermansia* may be positively correlated with inflammation [28]. Significant *Akkermansia* enrichment was also found in the intestines of Parkinson disease (PD) patients, which may be related to their proinflammatory state and recurrent gastrointestinal disease [29]. Our study revealed the upregulation of *Akkermansia* expression, suggesting that this may exert an anti-inflammatory effect in peripheral nerve xenotransplantation. A study noted the upregulation of Th1–Th17–Th22 Foxp3+ cells in the spleen of peripheral nerve xenotransplant recipients, suggesting that this Treg subpopulation is involved in mediating graft rejection [22]. Tregs play an important role in preventing GVHD, allograft rejection, and autoimmune disease [30,31]. Interestingly, the administration of *Akkermansia* to high-fat-diet-fed mice showed improved glucose tolerance and an increased number of goblet cells and adipose tissue-resident CD4 Foxp3+ Tregs [32], indicating *Akkermansia* might recruit Tregs in the host immune response following xenotransplantation. *Desulfovibrio* is predominant member of sulfate-reducing bacteria in human gut microbiota that produces a high concentration of lipopolysaccharide (LPS) [33]. The expression level of *Desulfovibrio* spp. and LPS were reported as both significantly
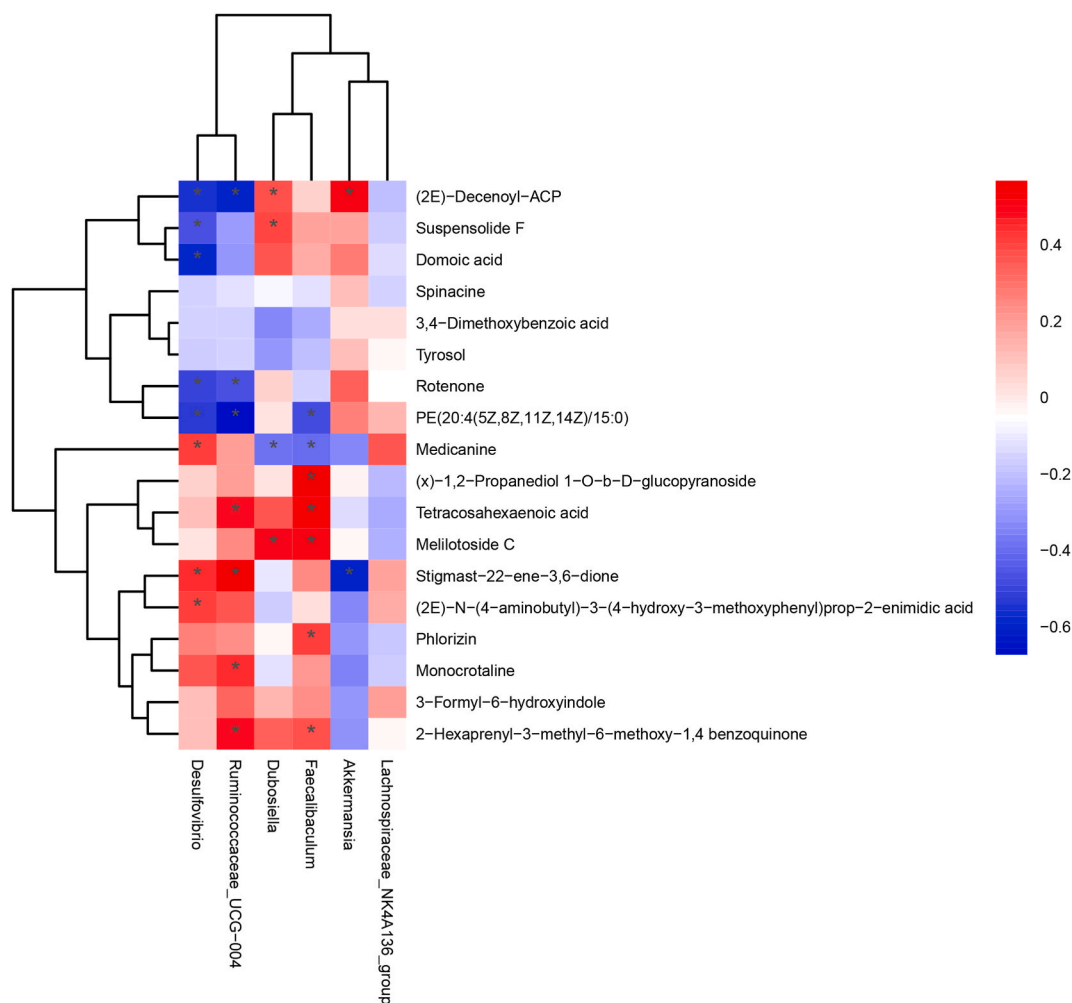
Fig. 6. Heatmap showing a significant correlation between different flora and differentially expressed metabolites after peripheral nerve xenotransplantation. The color scale bar ranges from −0.6 to 0.4, with blue, white, and red representing low (green), medium (black), and high (red) gene expression levels, respectively. (For interpretation of the references to color in this figure legend, the reader is referred to the Web version of this article.)

increased in liver injury mice [34]. In peripheral axotomy, overexpressed toll-like receptor 4 stimulated by LPS results in increased astrocytes and microglia response, involved in the process of synaptic remodeling, and affects the motoneuronal regenerative response and functionality [35]. Our study found that the expression level of *Desulfovibrio* significantly increased 1 month after surgery and decreased 3 months after surgery, suggesting that the upregulated *Desulfovibrio* may initiate host immunity against transplantation-related injuries and then become depleted during this process.

The intestinal microbiota degrades dietary fiber and produces a large number of SCFAs, the main components of which are acetate, propionate, and butyrate [36]. SCFAs are considered an important medium for maintaining intestinal homeostasis by regulating different cells [37–40]. Butyrate, an SCFA produced by the gut microbiota, was reported to play a role in exerting anti-inflammatory activity by inhibiting NF-κB signaling and increasing IL-10 expression [41]. The higher abundance of butyrate-producing bacteria increases the resistance of patients to lower respiratory tract viral infections and improves the prognosis of patients [42,43]. *Lachnospiraceae* and *Ruminococcaceae*, belonging to the *Clostridiales* order (*Firmicutes*), produce butyrate [44]. In this study, the expression level of *Lachnospiraceae* and *Ruminococcaceae* remained high at 1 month after transplantation, suggesting that they produce SCFAs and exert anti-inflammatory effects in the early period after peripheral nerve xenotransplantation. The expression levels of *Lachnospiraceae* and *Ruminococcaceae* were lower at 3 months after surgery compared with 1 month after surgery. This suggests that the regulatory effect of butyrate-producing microbiota is affected by the loss of nutrition and disturbance of the acid–base balance in the late period after peripheral nerve xenotransplantation. Possible factors affecting SCFA secretion are as follows: 1) the use of amino acids or proteins as alternative energy sources by bacteria to produce SCFAs when fermentable dietary fiber is severely depleted in a pathological state; and 2) the effect of pH on SCFA secretion [45]. The differentially expressed SCFAs may further affect bacterial levels by regulating the immune system.

Metabolites produced by microbiomes are considered key metabolic regulators that lead to a series of beneficial or harmful responses. Thus, it is meaningful to determine the relationships between microbiomes and their metabolites. We used nontargeted metabolomics analysis to detect the differential expression of metabolites and identified several that had a strong relationship with specific microorganisms, including (2E)-decenoyl-ACP, suspensolide F, rotenone, PE(20:4(5Z, 8Z, 11Z, 14Z)/15:0), medicanine, THA, melilotoside C, stigmast-22-ene-3,6-dione, and 2-hexaprenyl-3-methyl-6-methoxy-1,4 benzoquinone. Rotenone was suggested as one of the environmental neurotoxins implicated in PD etiopathogenesis [46,47]. THA is thought to be the immediate precursor of docosahexaenoic acid and plays a critical role in promoting n-3 polyunsaturated fatty acid biosynthesis [48,49], while 2-hexaprenyl-3--methyl-6-methoxy-1,4 benzoquinone is involved in antimicrobial activities [50].

In this study, we revealed that the relationship between fecal microbial flora and its metabolites may modulate host immune response in nerve transplantation. However, our findings are limited because no SCFAs were detected in the fecal metabolites. This may be because the concentration of SCFAs is too low to detect using nontargeted metabolomics analysis and requires targeted metabolomics analysis. Furthermore, samples of intestinal contents, instead of feces, may be required. Despite these limitations, our findings provide new insights into the mechanism of complications in peripheral nerve transplantation. We will compare differences in gut microbiota between allogeneic transplantation and xenotransplantation.

Our study found lower gut microbiome diversity with increased SCFA-producing microbiota and sulfate-reducing bacteria 1 month after peripheral nerve xenotransplantation, and these levels decreased 3 months after xenotransplantation. Additionally, the detection of specific bacterial metabolites is essential for identifying potential diagnostic markers for allograft rejection or characterizing therapeutic targets to prevent post-transplant infection.

Author contribution statement

Yongsheng Chen: Conceived and designed the experiments; Performed the experiments; Wrote the paper.
Shaopeng Li: Conceived and designed the experiments.
Huihui Chai, Zhenzhen Li, Bin Liu, Minxuan Tan, and Yanxia Ma: Conceived and designed the experiments; Analyzed and interpreted the data; Contributed reagents, materials, analysis tools or data.

Data availability statement

Data will be made available on request.

Ethics approval statement

The experiment was approved by the ethical committee of Guangzhou Forevergen Biosciences (Guangzhou, China) (approval number: IACUC-AEWC-F2006012).

Declaration of competing interest

The authors declare that they have no known competing financial interests or personal relationships that could have appeared to influence the work reported in this paper.

Appendix A. Supplementary data

Supplementary data to this article can be found online at https://doi.org/10.1016/j.heliyon.2023.e18529.

References

[1] X. Gu, et al., Construction of tissue engineered nerve grafts and their application in peripheral nerve regeneration, Prog. Neurobiol. 93 (2) (2011) 204–230.
[2] C.M. Nichols, et al., Effects of motor versus sensory nerve grafts on peripheral nerve regeneration, Exp. Neurol. 190 (2) (2004) 347–355.
[3] S. Panseri, et al., Electrospun micro- and nanofiber tubes for functional nervous regeneration in sciatic nerve transections, BMC Biotechnol. 8 (2008) 39.

[4] D. Muir, The potentiation of peripheral nerve sheaths in regeneration and repair, Exp. Neurol. 223 (1) (2010) 102–111.
[5] T. Lu, et al., Xenotransplantation: current status in preclinical research, Front. Immunol. 10 (2019) 3060.
[6] C. Wang, Q. Li, J. Li, Gut microbiota and its implications in small bowel transplantation, Front. Med. 12 (3) (2018) 239–248.
[7] A.S. Ismail, et al., Gammadelta intraepithelial lymphocytes are essential mediators of host-microbial homeostasis at the intestinal mucosal surface, Proc. Natl. Acad. Sci. U. S. A. 108 (21) (2011) 8743–8748.
[8] M. Schirmer, et al., Linking the human gut microbiome to inflammatory cytokine production capacity, Cell 167 (4) (2016) 1125–1136.e8.
[9] A.L. Hartman, et al., Human gut microbiome adopts an alternative state following small bowel transplantation, Proc. Natl. Acad. Sci. U. S. A. 106 (40) (2009) 17187–17192.
[10] K.J. Dery, et al., Microbiota in organ transplantation: an immunological and therapeutic conundrum? Cell. Immunol. 351 (2020), 104080.
[11] M. Ardalan, S.Z. Vahed, Gut microbiota and renal transplant outcome, Biomed. Pharmacother. 90 (2017) 229–236.
[12] Y. Shono, M.R.M. van den Brink, Gut microbiota injury in allogeneic haematopoietic stem cell transplantation, Nat. Rev. Cancer 18 (5) (2018) 283–295.
[13] J.U. Peled, et al., Microbiota as predictor of mortality in allogeneic hematopoietic-cell transplantation, N. Engl. J. Med. 382 (9) (2020) 822–834.
[14] M. Burgos da Silva, et al., Preservation of the fecal microbiome is associated with reduced severity of graft-versus-host disease, Blood 140 (22) (2022) 2385–2397.
[15] F. Noor, et al., The gut microbiota and hematopoietic stem cell transplantation: challenges and potentials, J. Innate Immun. 11 (5) (2019) 405–415.
[16] W. Ouyang, J.K. Kolls, Y. Zheng, The biological functions of T helper 17 cell effector cytokines in inflammation, Immunity 28 (4) (2008) 454–467.
[17] N. Köhler, R. Zeiser, Intestinal microbiota influence immune tolerance post allogeneic hematopoietic cell transplantation and intestinal GVHD, Front. Immunol. 9 (2018) 3179.
[18] S. Choi, P. Reddy, Graft-versus-host disease, Panminerva Med. 52 (2) (2010) 111–124.
[19] J.C. Fischer, et al., RIG-I/MAVS and STING signaling promote gut integrity during irradiation- and immune-mediated tissue injury, eaag2513, Sci. Transl. Med. 9 (386) (2017).
[20] P.V. Chang, et al., The microbial metabolite butyrate regulates intestinal macrophage function via histone deacetylase inhibition, Proc. Natl. Acad. Sci. U. S. A. 111 (6) (2014) 2247–2252.
[21] R. Tomasi, et al., T-cell response in a cardiac xenotransplant model, Exp. Clin. Transp. 19 (7) (2021) 708–716.
[22] H. Chai, et al., Decreased percentages of regulatory T cells are necessary to activate Th1-Th17-Th22 responses during acute rejection of the peripheral nerve xenotransplantation in mice, Transplantation 98 (7) (2014) 729–737.
[23] W. Wang, et al., Gut microbiota and allogeneic transplantation, J. Transl. Med. 13 (2015) 275.
[24] O. Storrø, E. Avershina, K. Rudi, Diversity of intestinal microbiota in infancy and the risk of allergic disease in childhood, Curr. Opin. Allergy Clin. Immunol. 13 (3) (2013) 257–262.
[25] G.A. Weiss, T. Hennet, Mechanisms and consequences of intestinal dysbiosis, Cell. Mol. Life Sci. 74 (16) (2017) 2959–2977.
[26] S. Astbury, et al., Lower gut microbiome diversity and higher abundance of proinflammatory genus Collinsella are associated with biopsy-proven nonalcoholic steatohepatitis, Gut Microb. 11 (3) (2020) 569–580.
[27] T. Zhang, et al., Akkermansia muciniphila is a promising probiotic, Microb. Biotechnol. 12 (6) (2019) 1109–1125.
[28] H. Ge, et al., Egg white peptides ameliorate dextran sulfate sodium-induced acute colitis symptoms by inhibiting the production of pro-inflammatory cytokines and modulation of gut microbiota composition, Food Chem. 360 (2021), 129981.
[29] S. Romano, et al., Meta-analysis of the Parkinson's disease gut microbiome suggests alterations linked to intestinal inflammation, NPJ Parkinsons Dis. 7 (1) (2021) 27.
[30] M. Romano, et al., Treg therapy in transplantation: a general overview, Transpl. Int. 30 (8) (2017) 745–753.
[31] T. Vaikunthanathan, et al., Regulatory T cells: tolerance induction in solid organ transplantation, Clin. Exp. Immunol. 189 (2) (2017) 197–210.
[32] N.R. Shin, et al., An increase in the Akkermansia spp. population induced by metformin treatment improves glucose homeostasis in diet-induced obese mice, Gut 63 (5) (2014) 727–735.
[33] A. Edlund, et al., Extractable and lipopolysaccharide fatty acid and hydroxy acid profiles from Desulfovibrio species, J. Lipid Res. 26 (8) (1985) 982–988.
[34] G. Xie, et al., Distinctly altered gut microbiota in the progression of liver disease, Oncotarget 7 (15) (2016) 19355–19366.
[35] P. Ribeiro, et al., Toll-like receptor 4 (TLR4) influences the glial reaction in the spinal cord and the neural response to injury following peripheral nerve crush, Brain Res. Bull. 155 (2020) 67–80.
[36] J.H. Cummings, Fermentation in the human large intestine: evidence and implications for health, Lancet 1 (8335) (1983) 1206–1209.
[37] M. Sun, et al., Microbiota-derived short-chain fatty acids promote Th1 cell IL-10 production to maintain intestinal homeostasis, Nat. Commun. 9 (1) (2018) 3555.
[38] Y. Zhao, et al., GPR43 mediates microbiota metabolite SCFA regulation of antimicrobial peptide expression in intestinal epithelial cells via activation of mTOR and STAT3, Mucosal Immunol. 11 (3) (2018) 752–762.
[39] L. Chen, et al., Microbiota metabolite butyrate differentially regulates Th1 and Th17 cells' differentiation and function in induction of colitis, Inflamm. Bowel Dis. 25 (9) (2019) 1450–1461.
[40] P.M. Smith, et al., The microbial metabolites, short-chain fatty acids, regulate colonic Treg cell homeostasis, Science 341 (6145) (2013) 569–573.
[41] M.A. Vinolo, et al., Regulation of inflammation by short chain fatty acids, Nutrients 3 (10) (2011) 858–876.
[42] J.U. Peled, et al., Intestinal microbiota and relapse after hematopoietic-cell transplantation, J. Clin. Oncol. 35 (15) (2017) 1650–1659.
[43] B.W. Haak, et al., Impact of gut colonization with butyrate-producing microbiota on respiratory viral infection following allo-HCT, Blood 131 (26) (2018) 2978–2986.
[44] C. Martin-Gallausiaux, et al., Butyrate produced by commensal bacteria down-regulates indolamine 2,3-dioxygenase 1 (Ido-1) expression via a dual mechanism in human intestinal epithelial cells, Front. Immunol. 9 (2018) 2838.
[45] C. Martin-Gallausiaux, et al., SCFA: mechanisms and functional importance in the gut, Proc. Nutr. Soc. 80 (1) (2021) 37–49.
[46] M. Badruzzaman, et al., Rotenone alters behavior and reproductive functions of freshwater catfish, Mystus cavasius, through deficits of dopaminergic neurons in the brain, Chemosphere 263 (2021), 128355.
[47] Y.J. Niu, et al., Melatonin enhances mitochondrial biogenesis and protects against rotenone-induced mitochondrial deficiency in early porcine embryos, J. Pineal Res. 68 (2) (2020), e12627.
[48] A.H. Metherel, et al., Docosahexaenoic acid is both a product of and a precursor to tetracosahexaenoic acid in the rat, J. Lipid Res. 60 (2) (2019) 412–420.
[49] A.H. Metherel, R.P. Bazinet, Updates to the n-3 polyunsaturated fatty acid biosynthesis pathway: DHA synthesis rates, tetracosahexaenoic acid and (minimal) retroconversion, Prog. Lipid Res. 76 (2019), 101008.
[50] E.N. Carcamo-Noriega, et al., 1,4-Benzoquinone antimicrobial agents against Staphylococcus aureus and Mycobacterium tuberculosis derived from scorpion venom, Proc. Natl. Acad. Sci. U. S. A. 116 (26) (2019) 12642–12647.